Probing the evolutionary robustness of anti-virulence treatments targeting iron uptake in *Pseudomonas aeruginosa*

Chiara Rezzoagli[1, *], David Wilson[1], Michael Weigert[1], Stefan Wyder[1], Rolf Kümmerli[1, *]

[1] Department of Plant and Microbial Biology, University of Zurich, Zurich, Switzerland

* Corresponding authors:

Email: chiara.rezzoagli@uzh.ch (CR), rolf.kuemmerli@uzh.ch (RK)

Abstract

Antivirulence treatments are therapeutic strategies that inhibit the expression or functioning of bacterial virulence factors. They hold great promise to be both effective and exert weaker selection for resistance than conventional antibiotics. However, the evolutionary robustness argument, based on the idea that anti-virulence treatments disarm rather than kill pathogens, is controversial, and there is a lack of studies testing the potential for resistance evolution under conditions relevant for infections. Here, we approach this issue by probing the evolutionary robustness of two anti-virulence treatments, gallium and flucytosine, targeting the iron scavenging pyoverdine of the opportunistic human pathogen *Pseudomonas aeruginosa*. We first let bacteria evolve under different drug concentrations in replicated populations over 20 days, using human serum as an ex-vivo model. We then applied a combination of phenotypic and genotypic screens to show that resistance against flucytosine quickly arose and spread in all populations. Genetic analysis revealed that mutations in *upp*, a gene encoding an enzyme required for flucytosine activation, are responsible for resistance evolution. Conversely, resistance against gallium arose only sporadically and not in all populations. Resistance mechanisms were based on mutations in transcriptional regulators, which resulted in the upregulation of pyocyanin, a redox-active molecule promoting siderophore-independent iron acquisition. Our work highlights that mutants resistant against anti-virulence treatments can easily arise, however, selective spreading varies considerably between treatments. This demonstrates that there is no ‘yes’ or ‘no’ answer to the question of whether anti-virulence treatments are evolutionarily robust. Instead, evolutionary robustness is a relative measure on a sliding scale, with specific treatments occupying different positions on this scale.

Author Summary

There is an urgent need for alternative therapeutic options against multi-drug resistant bacteria. Antivirulence approaches, which target bacterial virulence factors thereby

reducing the ability to establish and maintain infections, are proposed as an evolutionary robust way to manage infections. Conversely to conventional antibiotics, there is great hope that “disarming” rather than killing pathogens will exert weaker selection for resistance. Here we compared the evolutionary robustness of two proposed antivirulence drugs, gallium and flucytosine, both targeting the pyoverdine mediated iron-uptake in the opportunistic human pathogen *Pseudomonas aeruginosa*. Pyoverdine is a strong iron chelator and an important virulence factor during acute infections, and has thus been identified as a promising target for antivirulence drugs. After exposing bacteria to treatments for 20 days in human blood serum, as an *ex-vivo* infection model, we found that resistant mutants against the two anti-virulence drugs readily arose. However, extensive selective spreading of resistant clones was only observed for flucytosine but not for gallium treatment. Our study demonstrates that anti-virulence treatments are not evolutionarily robust *per se*, but vary substantially in their propensity to select for resistance. We thus need standardized protocols to identify those treatments that are both efficient in controlling infections and withstand resistance evolution.

Introduction

There is currently much interest in therapeutic approaches that inhibit the expression or functioning of bacterial virulence factors [1–8]. Virulence factors are structures and molecules that allow bacteria to establish and maintain infections, and to cause host damage [9,10]. Examples of virulence factors include flagella and pili to adhere to the host tissue, secreted enzymes, tissue-damaging toxins and siderophores to scavenge iron from the host [11]. Approaches that target these traits are called anti-virulence treatments. There is great hope that disarming rather than directly killing pathogens is an efficient and evolutionarily robust way to manage infections [2,12–15]. In particular, it is thought that anti-virulence treatments exert weaker selection for resistance than conventional antibiotics because pathogens are not killed directly. However, empirical evidence for the evolutionary robustness of anti-virulence treatments is controversial with positive and negative reports

currently balancing each other out [16–21]. Part of the controversy is that it remains unclear what a resistance phenotype is with regard to anti-virulence therapies, and that there is a shortage of studies examining resistance evolution under realistic conditions in parallel replicates both at the phenotypic and genetic level.

Here, we tackle this issue by probing the evolutionary robustness of two proposed anti-virulence treatments, gallium and flucytosine, using them as experimental test cases to demonstrate how resistance evolution can be examined and quantified. The two anti-virulence drugs target both the iron-scavenging pyoverdine of the opportunistic human pathogen *Pseudomonas aeruginosa* [19,22,23], which is an important virulence factor for this species during acute infections [19,24–30]. In the context of infections, the host actively withholds iron from pathogens by binding it to strong iron-chelating proteins, such as transferrin or lactoferrin [31]. In order to scavenge iron from these sources, opportunistic pathogenic bacteria secrete siderophores with high affinity for this essential nutrient. Given the importance of iron for bacterial growth, it has been proposed that drugs interfering with iron uptake could be effective therapeutics to control infection [32]. Gallium and flucytosine both fulfill this role, albeit through different modes of action. Gallium is an iron-mimic and binds irreversibly to pyoverdine outside the cell, thereby rendering the secreted molecules useless for iron uptake [19,22,30]. While gallium is an anti-virulence drug at low dosages, it can function as an antibiotic at high concentrations. Then, gallium penetrates into bacterial cells, where it is thought to replace iron in enzymes such as catalases and cytochromes, leading to cell death [33,34]. Flucytosine, meanwhile, is an anti-fungal drug that was repurposed for the use against bacterial pathogens [23]. This drug enters the pathogen, where it is enzymatically activated to a fluorinated ribonucleotide. This active form is then incorporated in the RNA and inhibits, via a yet unknown mechanism, the *pvdS* iron starvation sigma factor controlling pyoverdine synthesis [23,35].

Different lines of reasoning have been advocated for why these two drugs should be evolutionarily robust. Flucytosine, while stalling pyoverdine production, does not seem to compromise the growth of *P. aeruginosa* in in-vitro cultures [23]. If growth of the pathogen is not affected, evolutionary theory predicts that resistant mutants, resuming virulence factor production, should not experience a selective advantage and thus should not spread [15]. This reasoning for evolutionary robustness should not apply to gallium, which has been shown to compromise bacterial growth due to the induced iron starvation [19,22,36,37]. Conversely, gallium and also flucytosine are supposed to be evolutionarily robust because they suppress either the functioning (gallium) or the synthesis (flucytosine) of a secreted virulence factor, which can be shared as a public good between pathogen individuals (iron-loaded pyoverdine can be taken up by all bacteria with a matching receptor; [38,39]). Resistant mutants should not spread in this case because they bear the cost of resumed virulence factor production, whereas the benefit of increased virulence factor availability is shared with everyone else in the population, including the drug-susceptible individuals [12,14,16,20]. In addition, gallium is supposed to be evolutionarily robust because it targets a secreted virulence factor outside the cell. The reasoning here is that common resistance mechanisms, such as the prevention of drug influx, increased drug efflux, and intra-cellular drug degradation cannot operate outside the cell. Thus, an extra-cellular mode of drug action is supposed to reduce the number of mutational targets that can confer resistance [19].

To probe whether these principles apply to gallium and flucytosine, we exposed replicated populations of *P. aeruginosa* to two different concentrations of these two drugs in human blood serum. Together with a drug-free control treatment, we let the treated populations evolve for 20 consecutive days in eight-fold replication, by transferring a fraction of the evolving cultures to fresh human serum on a daily basis. Human serum has recently been established as an *ex-vivo* model to mimic realistic host conditions, as for instance experienced during bloodstream infections [40]. Following experimental evolution, we

screened evolved populations and randomly isolated clones for the evolution of resistance phenotypes. We focused on three potential resistance phenotypes, which include the (partial or full) restoration of growth, the (partial or full) restoration of virulence factor production, or the evolution of a bypassing mechanism for iron uptake [15,19]. Finally, we sequenced the whole genome of evolved clones to uncover the genetic basis of potential resistance mechanisms.

Results

Gallium and flucytosine affect both growth and pyoverdine production in human serum.

Since human serum is a novel *ex-vivo* model in the context of anti-virulence experiments, we first assessed whether (a) pyoverdine production is beneficial in this media, and (b) how gallium and flucytosine treatment affects the growth and pyoverdine production of *P. aeruginosa*. To test (a), we compared the growth of our wildtype strain PAO1 to its siderophore-negative mutants PAO1 Δ*pvdD* (deficient for pyoverdine production) and PAO1 Δ*pvdD* Δ*pchEF* (deficient for the production of pyoverdine and the secondary siderophore pyochelin) in human serum across a range of iron limitations (S1 Fig). Across all conditions, we observed that growth was significantly reduced in the siderophore-deficient mutants compared to the wildtype (ANOVA for PAO1 Δ*pvdD*: t_{49}= -8.13, $p < 0.0001$, for PAO1 Δ*pvdD* Δ*pchEF*: t_{49}= -7.92, $p < 0.0001$), confirming that human serum is an iron-limited media, and that pyoverdine is important for growth.

To test (b), we subjected PAO1 cultures to a range of drug concentrations under standardized conditions. The resulting dose-response curves reveal that both drugs significantly reduce bacterial growth (Fig 1A and 1B). For gallium, growth reduction manifested only at relatively high concentrations, whereas already the lowest concentration

of flucytosine caused a substantial growth reduction, which then remained fairly constant across the concentration gradient. This experiment further confirmed that both drugs affect the production of pyoverdine (Fig 1C and 1D), consistent with previous findings in standard laboratory media. For flucytosine, the lowest concentration tested completely stalled pyoverdine production. Gallium treatment affected pyoverdine production in a more complex way, but consistent with previous findings [19]: at intermediate gallium concentrations, pyoverdine is up-regulated to compensate for the gallium-induced pyoverdine inhibition, and down-regulated at higher concentrations, when pyoverdine-mediated signaling becomes impaired [22]. Our results thus reveal that both drugs affect pyoverdine production in the predicted way in human serum, and thus act as anti-virulence drugs.

Do bacteria evolve population-level resistance to antivirulence treatments?

We carried out an experimental evolution with eight independent lines per treatment for a period of 20 days, with daily transfers of a sub-fraction of the evolved cultures to fresh human serum. Our experimental design comprised five treatment regimes: a no-drug control treatment, a low and a high concentration treatment for both gallium and flucytosine. The concentrations used (50 μM and 280 μM for gallium and 10 μg/ml and 140 μg/ml for flucytosine) were inferred from the dose-response curves (Fig 1). Following experimental evolution, we measured whether evolved populations showed a resistance phenotype either through recovery of growth and/or a restoration of the pyoverdine production profile under the treatment regimes they evolved in. For growth (Fig 2A), we found that the evolved lines all grew significantly better than the treated ancestral wildtype (Welch's two sample t-tests, for gallium low: $t_{11.9} = -4.96$, $p = 0.0003$; for gallium high: $t_{13.3} = -6.48$, $p < 0.0001$; for flucytosine low: $t_{12.2} = -5.09$, $p = 0.0002$; for flucytosine high $t_{7.5} = -11.79$, $p < 0.0001$).

Regarding pyoverdine profiles, we observed no significant restoration of pyoverdine production for the lines evolved under low gallium concentration (comparison with the treated

ancestor, Welch's two sample t-test: $t_{8.8}$ = 0.94, p = 0.3719) (Fig 2B). Conversely, lines evolved under the other three drug regimes all showed a significant increase in pyoverdine production relative to the treated ancestor (Fig 2B) (Welch's two sample t-test for gallium high: $t_{13.1}$ = -3.69, p = 0.0026; for flucytosine low: $t_{7.2}$ = -7.64, p = 0.0001; for flucytosine high: $t_{9.6}$ = -54.65, p < 0.0001). While the increase was moderate for the gallium high treatment, there was full restoration of pyoverdine production in both flucytosine treatments (no significant difference relative to the ancestral untreated wildtype, ANOVA for flucytosine low: t_{88} = -1.31, p = 0.1944; for flucytosine high: t_{88} = 0.42, p = 0.6766).

Next, we asked whether the observed restoration of growth and pyoverdine production indeed indicates resistance evolution, or whether these patterns could also be explained by media adaptation. For that purpose, we analyzed the growth and pyoverdine production of lines evolved in the absence of drugs. We found that these control lines also showed a significant increase in pyoverdine production relative to the untreated ancestor (Welch's two sample t-test, $t_{9.1}$= -4.03, p = 0.0047, Fig 2B). Moreover, some of the untreated evolved lines also showed significantly improved growth, although the overall growth increase across lines was not significant ($t_{9.1}$ = -1.61, p = 0.1424, Fig 2A). These analyses demonstrate the difficulty of identifying resistance profiles of non-killing anti-virulence treatments, as it is hard to disentangle resistance evolution from media adaptation at the level of the entire population.

Screening for resistance profiles in evolved single clones

A more detailed way of screening for resistance profiles is to pick individual clones and measure whether their drug dose-response changed compared to the ancestor. In a first step, we thus isolated five random clones from each evolved line (i.e. 40 per treatment), and individually analyzed their growth and pyoverdine production. These analyses revealed high variation among clones in both growth and pyoverdine production in human serum (S2 Fig),

suggesting that most evolved populations were heterogeneous, consisting of multiple different genotypes. For in-depth analysis, we then randomly picked 16 single clones (four per drug treatment) and tested whether these evolved clones differ in their drug dose response curve compared to the ancestral wildtype.

We observed that three out of eight clones subjected to gallium (Fig 3A-3D) and all eight clones subjected to flucytosine showed a significantly altered dose response (Fig 3E-3H). Clones GL_2 and GL_3, evolved under low gallium, showed a significant increase in pyoverdine production under intermediate gallium concentrations (between 8 and 128 μM), which goes along with an improved growth performance for GL_2, but not GL_3. In contrast, clone GH_1, evolved under high gallium concentration, did not show an altered pyoverdine production response, but grew significantly better when exposed to gallium (Fig 3A-3D). For the eight clones evolved under the flucytosine regime, changes in the dose-response curves were both striking and uniform: growth and pyoverdine production were both no longer affected by the drug (Fig 3E-3H). Since these dose-response curve analyses directly include a control for media adaptation (i.e. the no-drug treatment), our results indicate that all eight clones evolved complete resistance to flucytosine. For gallium, on the other hand, our data suggest that three out of the eight clones exhibited a phenotype that is compatible with at least partial resistance.

Linking phenotypes to genotypes

To test whether there is a genetic basis for the putative resistance profiles described in Fig 3, we sequenced the whole genome of all 16 clones. Following read mapping to the PAO1 genome, we called sequence variants, both SNPs and INDELs, which have emerged during evolution under anti-virulence drug exposure (Table 1). For the clones evolved with flucytosine, we observed that all of them had acquired mutations in the coding sequence of *upp.* There were four different types of mutations, including two different non-synonymous

SNPs, a 15-bp deletion and a 1-bp insertion (S1 Table). The *upp* gene encodes for a uracil phosphoribosyl-transferase, which is one of the enzyme required for the activation of flucytosine in the cell [41,42].

For the clones evolved under gallium treatment, the mutational pattern was more heterogeneous (Table 1). While no mutations were detected for several clones (GH_2, GH_3, and GH_4), the three clones with significantly altered dose responses had indeed mutations that could be relevant in this context: clone GH_1 featured a 3-nt deletion in the coding sequence of *mvaU*, whereas the clones GL_2 and GL_3 were mutated in the *vfr* gene. Both *mvaU* and *vfr* encode transcriptional regulators involved in the regulation of virulence factor expression, including proteases, pyocyanin and pyoverdine.

In addition, several clones from the gallium and flucytosine treatments had mutations in either *dipA* (dispersion-induced phosphodiesterase A; GL_1, GL_4, FH_4) or *morA* (motility regulator; GL_3, FH_2). The repeated yet unspecific appearance of these mutations could suggest that they represent general adaptations to human serum. Taken together, our sequencing analysis identify three potential targets of selection that could be associated with resistance evolution: the gene *upp* for flucytosine, and the genes encoding for the global transcriptional virulence regulators *vfr* and *mvaU* for gallium. In the next section, we will investigate the possible underlying mechanisms of how mutations in these genes could confer resistance in more detail.

Table 1. List of mutations in evolved single clones.

Treatment	Clone	Gene[1]	Description	Mutation	Type	Position[2]
Gallium Low	GL_1	*dipA*	dispersion-induced phosphodiesterase A	CA→C	INDEL	5642855-5642856
	GL_2	*vfr*	transcriptional regulator	C→T	SNP	706108
	GL_3	*vfr*	transcriptional regulator	C→T	SNP	706108
		PA3801	conserved hypothetical protein	A→G	SNP	4260811
		morA	motility regulator	G→T	SNP	5158144
	GL_4	*dipA*	dispersion-induced phosphodiesterase A	CA→C	INDEL	5642855-5642856
Gallium High	GH_1	*mvaU*	transcriptional regulator	GAGC→G	INDEL	3016276-3016279
	GH_2	none				
	GH_3	none				
	GH_4	none				
Flucytosine Low	FL_1	*upp*	uracil phosphoribosyl-transferase	T→C	SNP	5213244
		yfiR	tripartite signaling complex	C→T	SNP	1214975
		PA1369	hypothetical protein	C→T	SNP	1483680
		PA2770-PA2771	intergenic region	G→A	SNP	3129202
	FL_2	*upp*	uracil phosphoribosyl-transferase	GAGAAGATCTCCGGGA→G	INDEL	5213011-5213037
	FL_3	*upp*	uracil phosphoribosyl-transferase	A→C	SNP	5212855
		upp	uracil phosphoribosyl-transferase	A→G	SNP	5213146
	FL_4	*upp*	uracil phosphoribosyl-transferase	T→C	SNP	5213244
		groEL	protein chaperone	G→A	SNP	4916838
		PA2770-PA2771	intergenic region	G→A	SNP	3129202
Flucytosine High	FH_1	*upp*	uracil phosphoribosyl-transferase	G→GC	INDEL	5212852
		upp	uracil phosphoribosyl-transferase	A→C	SNP	5212855
		fliF	flagella M-ring outer membrane protein precursor	CA→C	INDEL	1194060-1194061
	FH_2	*upp*	uracil phosphoribosyl-transferase	A→C	SNP	5212855
		morA	motility regulator	G→A	SNP	5159713
	FH_3	*upp*	uracil phosphoribosyl-transferase	A→C	SNP	5212855
		fliF	flagella M-ring outer membrane protein precursor	TCGTCC→T	INDEL	1193365-1193370
	FH_4	*upp*	uracil phosphoribosyl-transferase	A→C	SNP	5212855
		dipA	dispersion-induced phosphodiesterase A	GA→G	INDEL	5643059-5643060

[1]Only mutations not found in the ancestor wildtype PAO1 are reported. Common mutations among all samples and the ancestor are listed in S3 Table.

[2] Position on PAO1 reference genome

Evolution of bypassing mechanisms for iron acquisition under gallium treatment

Since gallium induces iron starvation via the quenching of pyoverdine molecules outside the cell, it was proposed that bacteria could evolve bypassing mechanisms to guarantee iron uptake in a siderophore-independent manner [19]. In human serum, where iron is bound to transferrin or heme, we can envisage two such bypassing mechanisms. First, bacteria could upregulate the production of pyocyanin, which can reduce ferric to ferrous iron outside the cell, thereby facilitating direct pyoverdine-independent iron uptake [18]. Second, bacteria could upregulate protease production to acquire iron from transferrin or heme through protease-induced hydrolysis [28,43]. To test whether such bypassing mechanisms evolved in our experiment, we quantified the production of pyocyanin and proteases in the eight clones evolved under gallium treatment.

We indeed found that three clones displayed significantly increased pyocyanin production per cell compared to the ancestral wildtype, and these were exactly the clones with mutations in either *mvaU* or *vfr* (Fig 4A; ANOVA for GH_1: $t_{79} = 9.64$, $p < 0.0001$; for GL_2: $t_{99} = 6.13$, $p < 0.0001$; for clone GL_3: $t_{99} = 14.8$, $p < 0.0001$). Since these clones are mutated in global transcriptional regulator *mvaU* or *vfr*, which control directly (*mvaU*) or indirectly (*vfr*) the expression of pyocyanin [44,45], a causal link between mutations in these genes and the observed increased pyocyanin production is likely. Hence, the upregulation of pyocyanin could represent a plausible by-passing mechanism, being under positive selection in the presence of gallium.

In contrast, we found little evidence that increased protease production could be an efficient by-passing mechanism in human serum. This is because six of the evolved clones actually showed reduced and not increased production of extracellular proteases (Fig 4B). Moreover, the two clones (GL_1 and GL_4) with significantly increased protease production

(ANOVA, for GL_1: $t_{10} = 13.22$, $p < 0.0001$; for GL_4: $t_{10} = 11.60$, $p < 0.0001$, Fig 4B) did not show an altered drug dose-response curve, suggesting that increased protease activity in these clones is not an evolutionary response to drug exposure.

Inactivation of Upp is responsible for resistance to flucytosine

As pointed out above, the enzyme Upp (uracil phosphoribosyl-transferase) is essential for the activation of flucytosine within the cell. The natural function of Upp is to convert uracil to UMP in the salvage pathway of pyrimidine (Fig 5A), with UMP representing a nucleotide precursor. Interestingly, *P. aeruginosa* can also produce UMP through the conversion of L-glutamine and L-aspartate [46] (Fig 5A). This multi-pronged metabolic network led us to hypothesize that *upp* might not be essential for the pyrimidine metabolism, and that the inactivation of this gene through mutations could confer resistance to flucytosine.

To test this hypothesis, we compared the flucytosine dose-response curve of the wildtype strain to an isogenic (transposon) mutant (MPAO1 Δ*upp*) with a non-functional *upp* gene. Consistent with the patterns of the evolved clones (Fig 3G), we found that MPAO1 Δ*upp* was completely insensitive to flucytosine: neither growth (Fig 5B) nor pyoverdine production (Fig 5C) were affected by the drug under the range of flucytosine concentration tested (Welch's two sample *t*-test for difference between wildtype and mutant, for growth: $t_{4.3} = -5.56$, $p = 0.0041$; for pyoverdine production: $t_{5.0} = -48.80$, $p < 0.0001$). These results strongly suggest that the inactivation of *upp* is a simple and efficient way to evolve resistance to flucytosine.

Discussion

New treatment approaches against the multi-drug resistant ESKAPE pathogens, to which *P. aeruginosa* belongs, are desperately needed [8,47,48]. In this context, anti-

virulence treatments that disarm rather than directly kill the bacteria have attracted particular interest, because such approaches have been proposed to be both effective in managing infections and sustainable in the sense that resistance should not easily evolve [2,5,12–15]. Promising approaches include the inhibition of quorum sensing molecules regulating virulence factor production [3], the suppression of toxins [49,50], or siderophore molecules required for iron-scavenging within the host [19,22,23,37,51]. In our study, we probed the evolutionary robustness argument by focusing on two anti-virulence drugs (gallium and flucytosine) targeting siderophore production of *P. aeruginosa*, as experimental test cases. Using a combination of replicated experimental evolution and phenotypic and genotypic analysis, our results do not support the unanimous argument for the evolutionary robustness of anti-virulence drugs currently prevailing in the literature. Instead, we found repeated and consistent evolution of complete resistance against flucytosine, based on a mechanism that prevents drug activation inside the cell. The situation is more promising for gallium, where different variants of partially resistant mutants, based on iron uptake bypassing mechanisms, only sporadically arose. Our work highlights that the question “are anti-virulence treatments evolutionarily robust?” cannot be answered with “yes” or “no”. Instead, we show that evolutionary robustness is a relative measure with specific treatments lying on different positions on the continuum between these two extremes. Our task is to assess the relative position of each novel treatment on this continuum.

Our work on flucytosine identifies two issues of anti-virulence approaches, which have been largely neglected so far. The first issue is that anti-virulence treatments can have considerable negative off-target effects, which turned out to be detrimental for the evolutionary robustness of flucytosine treatment (Fig 5A). Flucytosine undergoes several enzymatic modifications within the cell, finally resulting in fluorinated ribonucleotides, which compromise RNA and DNA functionality [52]. Thus, flucytosine not only inhibits pyoverdine synthesis, but likely compromises cell viability more generally, setting the stage for selection

to favor mutants with alleviated fitness costs under drug exposure. Our results support that exactly this scenario occurred during experimental evolution in human serum through mutations in *upp*. Fig 5A shows that the essential pyrimidine nucleotide precursor UMP can be synthesized through the salvage pathways reutilizing exogenous free bases and nucleosides, or via a *de novo* biosynthesis pathway using L-glutamine or L-aspartate. This latter pathway requires higher amounts of energy (phosphate and reducing power), and this is why organisms preferentially use the salvage pathway. However, the salvage pathway generates the harmful fluoro-UMP under flucytosine treatment, which provides a selective advantage to mutants that inhibit the salvage pathway (through mutations in *upp*) and switch to the *de novo* biosynthesis pathway. The second issue is that whether or not anti-virulence drugs affect pathogen fitness can depend on the ecological context. While Imperi et al. [23] showed that flucytosine does not significantly reduce bacterial growth in trypticase soy broth dialysate (TSBD), we demonstrate significant fitness effects of this drug in human serum. Although these variable outcomes might not be surprising from an ecological perspective, they have significant consequences for the evolutionary robustness argument of anti-virulence drugs: it may vary from one infectious context to another.

While flucytosine failed our hopes of evolutionary robustness, gallium is more promising because we observed no pervasive pattern of resistance evolution. Nonetheless, this anti-virulence treatment is not beyond any doubts, as we characterized several clones that have evolved putative bypassing mechanism through which gallium-mediated pyoverdine quenching can be circumvented. We found one evolved clone with a mutation in *mvaU*, encoding a positive regulator of pyocyanin production. This mutant indeed overproduced the redox-active molecule pyocyanin, which is able to reduce iron extracellularly, possibly promoting iron uptake in a pyoverdine-independent way [18]. We further isolated two independent clones with mutations in *vfr*, encoding a global virulence factor regulator [10]. These mutants showed generally increased pyocyanin expression (Fig 4A) and increased

pyoverdine production (Fig 3C) under drug exposure. The molecular interpretation of these patterns is that mutations in Vfr are known to stimulate PQS (Pseudomonas Quinolon Signal) synthesis, which is inhibited by a functional Vfr. PQS in turn is known to positively regulate pyocyanin synthesis. At the same time, it was shown that secreted PQS serves as an iron chelator, increasing iron limitation thereby promoting pyoverdine synthesis [45,53].

Important to note, however, is that the occurrence of resistant mutants alone does not necessarily mean that they spread and fix in the population. So, we might ask why mutants with *mvaU* or *vfr* were not more prevalent given their gallium-resistant phenotypes. One plausible evolutionary answer is that pyocyanin itself is secreted and might serve as a public good. Thus, the benefit of its action (reducing iron extracellularly) could be shared between resistant and susceptible wildtype cells. This scenario would corroborate the evolutionary argument that resistant mechanisms, which are based on public good traits, should not fix in a population [19,54–56]. This is a promising argument, supporting the idea that gallium is a relatively robust anti-virulence drug. Nonetheless, the down-side of our finding is that the putative by-passing mechanism observed involves the up-regulation of a potent toxin, which is itself considered a virulence factor [57]. While several studies have suggested that the quenching of particular virulence factors can lead to a phenotypic up-regulation of other regulatorily-linked virulence factors [30,58], we here show that the same can happen as a by-product of resistance evolution (as hypothesized by [59]). Whether and to what extent this pattern affects virulence in a host should receive particular attention in future studies.

By using a replicated experimental evolution design, combined with phenotypic and genetic analyses, our study helps to resolve the current debate in the literature on whether or not anti-virulence approaches are evolutionarily robust. The proponents of the evolutionary robustness argument relied so far on evolutionary theory and proof-of-principle studies to support their idea that putatively resistant mutants cannot invade population of susceptible

bacteria [14,16,19,20]. Their main argument is that resistant mutants, restoring virulence factor production, cannot spread because they alone carry the cost of virulence factor synthesis, whilst sharing the benefit with all cells in the population, including the susceptible ones. This prediction indeed held in competition experiments with engineered mimics of resistant mutants under well-mixed conditions, where virulence factors are easily shared [16,20]. Our experiments with gallium partially support their argument as mutants with up-regulated pyoverdine or pyocyanin production did neither seem to have fixed in populations (S2 Fig), nor did they appear in all replicates (Table 1). Nonetheless, *vfr* mutants for instance appeared independently in two replicates, which suggests that these mutants experienced a certain selective advantage. This advantage could be explained by the fact that human serum is a viscous medium limiting the diffusion of secreted compounds [60], such that *vfr*-mutants could experience a local advantage by increasing pyoverdine and pyocyanin production. The local advantage might allow them to increase to a certain frequency, potentially leading to a stable co-existence with the drug-susceptible wildtype strain. This phenomenon, known as negative-frequency dependent selection, has been described for several microbial public goods [54,61,62].

Conversely, the proponents of the argument that anti-virulence therapies are not evolutionarily robust rely on a number of experiments where mutants with resistant phenotypes were isolated [17,18,63,64]. Our experiments with flucytosine also support their line of argumentation, as we found pervasive resistance evolution against this treatment. This matches the results by Maeda et al. [17], who showed that resistance to the quorum-quenching compound C-30 (brominated furanone) evolves repeatedly via upregulation of a drug efflux pump. The spread of these mutants can be explained by the fact that their treatment did not solely interfere with quorum quenching but also compromised the ability of cells to grow in the adenosine medium, which requires a functional quorum sensing system [65]. Their study together with our work show that as soon as there are negative off-target

effects, affecting the fitness of individual cells, resistance mechanisms will arise and spread. Taken together, our study contributes to the solution of the debate by demonstrating that the details of the mode of action together with the ecological context determine whether and to what extent an anti-virulence drug can be evolutionarily robust.

In conclusion, our work advances research on anti-virulence drugs on multiple fronts. First, it shows that resistant phenotypes are difficult to define, as they can involve the restoration of growth, the resumption of virulence factor production, and/or the activation of a bypassing mechanism. Detailed phenotypic and genotypic analyses, as those proposed in our study, are required to disentangle background adaptation from resistance evolution. Second, we show that anti-virulence approaches are neither completely evolution-proof nor does the notion “all roads lead to resistance” apply [66]. A detailed evolutionary analysis for each individual drug is required to find out where it is situated on the continuum between the two extremes. Third, we advocate the application of more rigorous evolutionary approaches to test for resistance evolution. While there are rigorous standards when it comes to describing the precise molecular mode of action of a novel antibacterial [21,67], there is much room for improvement for standards regarding the quantification and characterization of resistance evolution [68,69].

Material and Methods

Strains and culturing conditions

We used the commonly used and genetically well-characterized *P. aeruginosa* PAO1 wildtype strain for all experiments. For some assays, we further used control strains, which are listed in S2 Table. Overnight cultures were grown in 8 ml Luria–Bertani (LB) medium in 50-ml Falcon tubes and incubated at 37°C, 200 rpm for 18 hours. For all experiments, we washed overnight cultures with 0.8% NaCl saline solution and adjusted them to OD_{600} = 2.5. Bacteria were further diluted to a final starting of $OD_{600} = 2.5 \times 10^{-3}$.

Growth assays in human serum

To understand to what extent iron is a limiting factor for bacterial growth in human serum (from Sigma-Aldrich, Switzerland), we grew PAO1 and the corresponding siderophore-deficient mutants in human serum supplemented with either: (a) 50 mM HEPES to buffer the medium at physiological pH; (b) 50 mM HEPES together with the strong iron chelator human apo-transferrin (100 µg/ml) and its co-factor $NaHCO_3$ (20 mM) to further increase iron limitation; or (c) 50 mM HEPES together with $FeCl_3$ 20µM to decrease iron limitation (S1 Fig). For the main experiments, we decided to use medium variant (b), representing the most strongly iron limited medium. All chemicals where purchased from Sigma-Aldrich, Switzerland.

Growth and virulence factor inhibition curves

We used gallium ($GaNO_3$) and flucytosine (5-Fluorocytosine) as anti-virulence drugs targeting pyoverdine production (purchased from Sigma-Aldrich). To assess the extent to which these two compounds inhibit PAO1 growth and pyoverdine production, we subjected bacterial cultures to a range of antibacterial concentrations. For each compound we tested 8 concentrations, which included 0, 8, 16, 32, 64, 128, 256, 512 µM and 0, 2.5, 5, 10, 20, 40, 80, 140 µg/ml for gallium and flucytosine, respectively. Overnight cultures of bacteria were

grown and diluted as described above and used to inoculate 200 µl of iron-limited human serum on 96-well plates. We then incubated the plates at 37 °C in a Tecan Infinite M-200 plate reader (Tecan Group Ltd., Switzerland), and tracked growth by measuring OD at 600 nm and pyoverdine-associated fluorescence (excitation at 400 nm, emission at 460 nm) every 15 minutes for 24 hours. Plates were shaken for 15 seconds (3 mm orbital displacement) prior to each reading event.

Experimental evolution

We exposed wildtype cultures of PAO1 to experimental evolution for a period of 20 days under five different selective regimes in eight-fold replication each. We had a no-drug control treatment in addition to a low and a high concentration drug treatment for both gallium and flucytosine. The concentrations used were inferred from the dose-response curves (Fig 1), and were 50 µM and 280 µM for gallium and 10 µg/ml and 140 µg/ml for flucytosine. Experimental evolution took place in 190 µl iron-limited human serum distributed on the inner wells of a 96-well plate. The plate also contained wells with media but no bacteria as negative media controls. To initiate experimental evolution, an overnight culture of PAO1 was grown as described above, and individual wells were inoculated with 10 µl of diluted culture to a final density of 10^6 cells per well (10^{-3} final dilution). The plate was incubated statically at 37°C in the plate reader for 23.5 hours, and OD_{600} was measured every 15 minutes prior to a shaking event (15 seconds at amplitude 3). After this growth period, cultures were appropriately diluted in 0.8% NaCl and transferred to a new plate containing fresh media. During the first 10 days of experimental evolution, the culture dilution factor was 10^{-3}. Because there was a general increase in culture growth over this time period, we increased culture dilution factor to $2*10^{-3}$ from day 11 to 20. Finally, to account for the fact that the positive controls (bacteria in human serum without treatments) grew better than the anti-bacterial treated cultures, we used dilution factors of $2*10^{-3}$ (from day 1 to 10) and $4*10^{-3}$

(from 11-20) for this treatment. Following each transfer, we preserved cultures by adding 100 µl of a 50% glycerol-LB solution, and storing the mixture at -80°C.

Population level resistance profiles

To test whether evolved populations had adapted to the presence of the antibacterials by restoring growth and/or pyoverdine production, we exposed all evolved lineages to the same drug concentration they experienced during experimental evolution, under standardized conditions in 5-fold replication each. To compare the performance of the evolved lineages relative to the ancestor wildtype, we simultaneously grew the wildtype under drug and no-drug treatments. Plates were incubated at 37° C, shaken at 160 rpm for 24 hours. Subsequently, we measured OD_{600} and pyoverdine-associated fluorescence using the plate reader, and scaled all values relative to the untreated wildtype.

Single clone isolation and inhibition curves

To isolate random clones from evolved lineages, we streaked out an aliquot of the final day freezer stocks of the experimental evolution onto LB plates. After overnight incubation at 37°C, we randomly picked five colonies from each evolved lineage (i.e. 200 clones in total). To assess the variation in growth and pyoverdine production of these evolved clones, we measured their performance under the treatment conditions they experienced during experimental evolution in 3-fold replication, in the same way we did for the population-level analysis. Moreover, we performed an in-depth analysis for 16 randomly picked single clones (four per drug treatment). In particular, we repeated the drug-inhibition experiments using the same concentrations and the identical protocol as described above for the ancestral wildtype.

Sequencing analysis

We isolated the genomic DNA of the 16 evolved clones and performed whole genome re-sequencing. We used the GenElute Bacterial Genomic DNA kit (Sigma Aldrich)

for DNA isolation. DNA concentrations were assayed using the Quantifluor dsDNA sample kit (Promega) and samples were sent to the Functional Genomics Center Zurich for library preparation (Nextera XT) and sequencing. Sequencing was performed on the Illumina HiSeq 4000 platform with single-end 125 base pair reads. Adapter sequences were clipped using Trimmomatic v0.33 [70] and reads trimmed using Flexbar v2.5 [71]. We then aligned the reads to the PAO1 reference genome using BWA v0.7.12 [72] and applied GATK v3.5 [73] indel realignment, duplicate removal and HaplotypeCaller SNP/INDEL discovery according to the GATK Best Practices recommendations, generating a variant call format (VCF) file, which was then filtered as following: (i) variants with coverage < 20 reads were discarded; (ii) variants with a Fisher Strand (FS) score > 30.0 were discarded to ensure there is no strand bias in the data; (iii) variants with a QD value < 2.0 were discarded (confidence value that there is a true variation at a given site); and (iv) clustered variants (≥ 3 variants in 35nt window) were discarded as they likely present sequencing or alignment artifacts. This filtering process yielded a list of potential SNPs and small INDELs, which we annotated using snpEff 4.1g [74] and then screened manually, compared to the sequenced genome of our ancestor wildtype for relevant mutations in gene coding and intergenic regions (see S3 Table).

Pyocyanin and protease assays

To establish links between the detected mutations and phenotypes, we screened the eight sequenced clones evolved under gallium for changes in their proteases and pyocyanin production profiles. To quantify pyocyanin production, we inoculated cells from overnight cultures (diluted to a starting of $OD_{600} = 10^{-6}$) into 1 ml of LB. Following incubation for 24 hours at 37°C under shaken conditions (160 rpm), we measured pyocyanin in the cell-free supernatant through absorbance at OD_{691} nm using the plate reader (protocol adapted from [19]). We further quantified protease production of the same eight clones in human serum (inoculated from overnight culture to a starting $OD_{600} = 2.5 \times 10^{-3}$). Following growth for 24

hours at 37°C under shaken conditions (160 rpm), we isolated the supernatants containing proteases through centrifugation of the cultures at 3700 rpm for 15 minutes. We then set up the proteolytic reaction mix (adapted from [75]) containing 0.1 ml of azocasein solution (30 mg/ml), 0.3 ml of 50 mM phosphate buffer (pH 7.5), and 0.1 ml culture supernatant. The samples were incubated at 37°C for 2 hours, during which hydrolysis of the azocasein releases the azo-dye, generating an absorbance signal at 366 nm, which is proportional to the proteolytic activity. The proteolytic reaction was stopped adding 0.5 ml 20% (w/v) trichloroacetic acid (TCA). We then centrifuged the mixture at 12000 rpm for 10 min, and quantified the proteolytic activity via absorbance reading in the plate reader.

Statistical analysis

Statistical analysis was carried out in RStudio (version 0.99.896, with R version 3.3.0). We analysed kinetic growth curves and pyoverdine production profiles using the *grofit* package [76]. Because growth patterns often followed non-logistic trajectories, we fitted non-parametric model (Splines) curves to estimate curve parameters, such as yield and integral (area under the curve). Integral is particularly useful in the context of non-parametric growth trajectories because it combines information on the lag-phase, growth rate and yield into one growth parameter. To analyse dose-response curves we used the *drc* package [77] version 3.0-1. Model selection was conducted by comparison of different non-linear models and the best fit was chosen using the following criteria: the log likelihood value, Akaike's information criterion (AIC), the estimated residual standard error and the *p*-value from a lack-of-fit test. It turned out that Weibull and Gompertz functions provided the best fit for gallium and flucytosin dose-response curves, respectively. For all analyses, we scaled growth and pyoverdine production relative to the untreated ancestral wildtype (=1). We used general linear mixed effect models to compare whether parameters of growth or pyoverdine profiles differ in evolved cultures treated with or without antibacterials. We further used Welch's two-sample *t*-test to compare whether growth and pyoverdine levels of evolved lines differ from the

ancestor wildtype. Statistical analysis of the dose-response curve for the evolved single clones was carried out by first fitting spline curves to the dose-response data, followed by the estimation of integrals for these spline fits, and the comparison of the scaled fits relative to the ancestor wildtype using a one-way ANOVA (Analysis of variance). Protease and pyocyanin production of evolved single clones and the ancestor wildtype were corrected for cell number (OD_{600}) and analysed using ANOVA.

Data availability

Whole-genome sequencing data have been deposited in the ArrayExpress database at EMBL-EBI (www.ebi.ac.uk/arrayexpress) under accession number E-MTAB-6110.

Acknowledgments

We thank Adin Ross-Gillespie for advice, and the Functional Genomics Center Zurich for technical support with the strain sequencing.

References

1. Escaich S. Antivirulence as a new antibacterial approach for chemotherapy. Curr Opin Chem Biol. 2008;12: 400–408. doi:10.1016/j.cbpa.2008.06.022
2. Rasko DA, Sperandio V. Anti-virulence strategies to combat bacteria-mediated disease. Nat Rev Drug Discov. 2010;9: 117–128. doi:10.1038/nrd3013
3. LaSarre B, Federle MJ. Exploiting Quorum Sensing To Confuse Bacterial Pathogens. Microbiol Mol Biol Rev. 2013;77: 73–111. doi:10.1128/MMBR.00046-12
4. Maura D, Ballok AE, Rahme LG. Considerations and caveats in anti-virulence drug development. Curr Opin Microbiol. 2016;33: 41–46. doi:10.1016/j.mib.2016.06.001
5. Vale PF, McNally L, Doeschl-Wilson A, King KC, Popat R, Domingo-Sananes MR, et al. Beyond killing. Evol Med Public Heal. 2016; 148–157. doi:10.1093/emph/eow012
6. Johnson BK, Abramovitch RB. Small Molecules That Sabotage Bacterial Virulence.

Trends Pharmacol Sci. 2017;38: 339–362. doi:10.1016/j.tips.2017.01.004

7. Rampioni G, Visca P, Leoni L, Imperi F. Drug repurposing for antivirulence therapy against opportunistic bacterial pathogens. Emerg Top Life Sci. 2017; doi:10.1042/ETLS20160018

8. Dickey SW, Cheung GYC, Otto M. Different drugs for bad bugs: antivirulence strategies in the age of antibiotic resistance. Nat Rev Drug Discov. 2017;16: 1–15. doi:10.1038/nrd.2017.23

9. Rahme LG, Stevens EJ, Wolfort SF, Shao J, Tompkins RG, Ausubel FM. Common virulence factors for bacterial pathogenicity in plants and animals. Science (80-). 1995;268: 1899–902. doi:10.1126/science.7604262

10. Balasubramanian D, Schneper L, Kumari H, Mathee K. A dynamic and intricate regulatory network determines Pseudomonas aeruginosa virulence. Nucleic Acids Res. 2013;41: 1–20. doi:10.1093/nar/gks1039

11. Wu HJ, Wang AHJ, Jennings MP. Discovery of virulence factors of pathogenic bacteria. Curr Opin Chem Biol. 2008;12: 93–101. doi:10.1016/j.cbpa.2008.01.023

12. André JB, Godelle B. Multicellular organization in bacteria as a target for drug therapy. Ecol Lett. 2005;8: 800–810. doi:10.1111/j.1461-0248.2005.00783.x

13. Baron C. Antivirulence drugs to target bacterial secretion systems. Curr Opin Microbiol. 2010;13: 100–105. doi:10.1016/j.mib.2009.12.003

14. Pepper JW. Drugs that target pathogen public goods are robust against evolved drug resistance. Evol Appl. 2012;5: 757–761. doi:10.1111/j.1752-4571.2012.00254.x

15. Allen RC, Popat R, Diggle SP, Brown SP. Targeting virulence: can we make evolution-proof drugs? Nat Rev Microbiol. 2014;12: 300–308. doi:10.1038/nrmicro3232

16. Mellbye B, Schuster M. The sociomicrobiology of antivirulence drug resistance: a proof of concept. MBio. 2011;2: e00131-11. doi:10.1128/mBio.00131-11

17. Maeda T, García-Contreras R, Pu M, Sheng L, Garcia LR, Tomás M, et al. Quorum quenching quandary: resistance to antivirulence compounds. ISME J. 2012;6: 493–

501. doi:10.1038/ismej.2011.122

18. García-Contreras R, Lira-Silva E, Jasso-Chávez R, Hernández-González IL, Maeda T, Hashimoto T, et al. Isolation and characterization of gallium resistant Pseudomonas aeruginosa mutants. Int J Med Microbiol. 2013;303: 574–582. doi:10.1016/j.ijmm.2013.07.009

19. Ross-Gillespie A, Weigert M, Brown SP, Kümmerli R. Gallium-mediated siderophore quenching as an evolutionarily robust antibacterial treatment. Evol Med Public Heal. 2014;2014: 18–29. doi:10.1093/emph/eou003

20. Gerdt JP, Blackwell HE. Competition Studies Confirm Two Major Barriers That Can Preclude the Spread of Resistance to Quorum-Sensing Inhibitors in Bacteria. ACS Chem Biol. 2014;9: 2291–2299. doi:10.1021/cb5004288

21. Sully EK, Malachowa N, Elmore BO, Alexander SM, Femling JK, Gray BM, et al. Selective Chemical Inhibition of agr Quorum Sensing in Staphylococcus aureus Promotes Host Defense with Minimal Impact on Resistance. PLoS Pathog. 2014;10. doi:10.1371/journal.ppat.1004174

22. Kaneko Y, Thoendel M, Olakanmi O, Britigan BE, Singh PK. The transition metal gallium disrupts Pseudomonas aeruginosa iron metabolism and has antimicrobial and antibiofilm activity. J Clin Invest. 2007;117: 877–888. doi:10.1172/JCI30783

23. Imperi F, Massai F, Facchini M, Frangipani E, Visaggio D, Leoni L, et al. Repurposing the antimycotic drug flucytosine for suppression of Pseudomonas aeruginosa pathogenicity. Proc Natl Acad Sci U S A. 2013;110: 7458–63. doi:10.1073/pnas.1222706110

24. Meyer JM, Neely A, Stintzi A, Georges C, Holder IA. Pyoverdin is essential for virulence of Pseudomonas aeruginosa. Infect. Immun. 1996. pp. 518–523.

25. Takase H, Nitanai H, Hoshino K, Otani T. Impact of siderophore production on Pseudomonas aeruginosa infections in immunosuppressed mice. Infect Immun. 2000;68: 1834–1839.

26. Harrison F, Browning LE, Vos M, Buckling A. Cooperation and virulence in acute Pseudomonas aeruginosainfections. BMC Biol. 2006;4: 21. doi:10.1186/1741-7007-4-21

27. Cornelis P, Dingemans J. Pseudomonas aeruginosa adapts its iron uptake strategies in function of the type of infections. Front Cell Infect Microbiol. 2013;3: 75. doi:10.3389/fcimb.2013.00075

28. Bonchi C, Imperi F, Minandri F, Visca P, Frangipani E. Repurposing of gallium-based drugs for antibacterial therapy. BioFactors. 2014;40: 303–312. doi:10.1002/biof.1159

29. Granato ET, Harrison F, Kümmerli R, Ross-Gillespie A. Do Bacterial “Virulence Factors” Always Increase Virulence? A Meta-Analysis of Pyoverdine Production in Pseudomonas aeruginosa As a Test Case. Frontiers in Microbiology. 2016. p. 1952. doi:https://doi.org/10.3389/fmicb.2016.01952

30. Weigert M, Ross-Gillespie A, Leinweber A, Pessi G, Brown SP, Kümmerli R. Manipulating virulence factor availability can have complex consequences for infections. Evol Appl. 2017;10: 91–101. doi:10.1111/eva.12431

31. Valenti P, Berlutti F, Conte MP, Longhi C, Seganti L. Lactoferrin Functions: Current Status and Perspectives. J Clin Gastroenterol. 2004;38: S127-9.

32. Smith DJ, Lamont IL, Anderson GJ, Reid DW. Targeting iron uptake to control Pseudomonas aeruginosa infections in cystic fibrosis. Eur Respir J. 2013;42: 1723–36. doi:10.1183/09031936.00124012

33. Chitambar CR. Gallium-containing anticancer compounds. Future Med Chem. 2012;4: 1257–1272. doi:10.4155/fmc.12.69

34. Hijazi S, Visca P, Frangipani E. Gallium-Protoporphyrin IX Inhibits Pseudomonas aeruginosa Growth by Targeting Cytochromes. Front Cell Infect Microbiol. 2017;7: 1–15. doi:10.3389/fcimb.2017.00012

35. Visca P, Imperi F, Lamont IL. Pyoverdine siderophores: from biogenesis to biosignificance. Trends Microbiol. 2007;15: 22–30. doi:10.1016/j.tim.2006.11.004

36. Banin E, Lozinski A, Brady KM, Berenshtein E, Butterfield PW, Moshe M, et al. The potential of desferrioxamine-gallium as an anti-*Pseudomonas* therapeutic agent. Proc Natl Acad Sci U S A. 2008;105: 16761–16766. doi:10.1073/pnas.0808608105

37. DeLeon K, Balldin F, Watters C, Hamood A, Griswold J, Sreedharan S, et al. Gallium Maltolate Treatment Eradicates Pseudomonas aeruginosa Infection in Thermally Injured Mice. Antimicrob Agents Chemother. 2009;53: 1331–1337. doi:10.1128/AAC.01330-08

38. Inglis RF, Scanlan P, Buckling A. Iron availability shapes the evolution of bacteriocin resistance in Pseudomonas aeruginosa. ISME J. 2016;10: 2060–2066. doi:10.1038/ismej.2016.15

39. Griffin AS, West SA, Buckling A. Cooperation and competition in pathogenic bacteria. Nature. 2004;430: 1024–1027. doi:10.1038/nature02744

40. Bonchi C, Frangipani E, Imperi F, Visca P. Pyoverdine and proteases affect the response of pseudomonas aeruginosa to gallium in human serum. Antimicrob Agents Chemother. 2015;59: 5641–5646. doi:10.1128/AAC.01097-15

41. Edlind TD, Katiyar SK. Mutational Analysis of Flucytosine Resistance in Candida glabrata. Antimicrob Agents Chemother. 2010;54: 4733–4738. doi:10.1128/AAC.00605-10

42. Beck DA, O'Donovan GA. Pathways of pyrimidine salvage in Pseudomonas and former Pseudomonas: Detection of recycling enzymes using high-performance liquid chromatography. Curr Microbiol. 2008;56: 162–167. doi:10.1007/s00284-007-9050-3

43. Doring G, Pfestorf M, Botzenhart K, Abdallah MA. Impact of Proteases on Iron Uptake of Pseudomonas aeruginosa Pyoverdin from Transferrin and Lactoferrin. 1988;56: 291–293.

44. Li C, Wally H, Miller SJ, Lu C. The multifaceted proteins MvaT and MvaU, members of the H-NS family, control arginine metabolism, pyocyanin synthesis, and prophage activation in Pseudomonas aeruginosa PAO1. J Bacteriol. 2009;191: 6211–6218.

doi:10.1128/JB.00888-09

45. Diggle SP, Matthijs S, Wright VJ, Fletcher MP, Chhabra SR, Lamont IL, et al. The Pseudomonas aeruginosa 4-Quinolone Signal Molecules HHQ and PQS Play Multifunctional Roles in Quorum Sensing and Iron Entrapment. Chem Biol. 2007;14: 87–96. doi:10.1016/j.chembiol.2006.11.014

46. Isaac JH, Holloway BW. Control of pyrimidine biosynthesis in Pseudomonas aeruginosa. J Bacteriol. 1968;96: 1732–41.

47. Pendleton JN, Gorman SP, Gilmore BF. Clinical relevance of the ESKAPE pathogens. Expert Rev Anti Infect Ther. 2013;11: 297–308. doi:10.1586/eri.13.12

48. Brown D. Antibiotic resistance breakers: can repurposed drugs fill the antibiotic discovery void? Nat Rev Drug Discov. 2015;14: 821–832. doi:10.1038/nrd4675

49. Lu C, Maurer CK, Kirsch B, Steinbach A, Hartmann RW. Overcoming the Unexpected Functional Inversion of a PqsR Antagonist in Pseudomonas aeruginosa□: An In Vivo Potent Antivirulence Agent Targeting pqs Quorum Sensing. Angew Chemie Int Ed. 2014;53: 1109–1112. doi:10.1002/anie.201307547

50. Henry BD, Neill DR, Becker KA, Gore S, Bricio-Moreno L, Ziobro R, et al. Engineered liposomes sequester bacterial exotoxins and protect from severe invasive infections in mice. Nat Biotechnol. 2015;33: 81–88. doi:10.1038/nbt.3037

51. Kelson AB, Carnevali M, Truong-Le V. Gallium-based anti-infectives: targeting microbial iron-uptake mechanisms. Curr Opin Pharmacol. 2013;13: 707–716. doi:10.1016/j.coph.2013.07.001

52. Harbers E, Chaudhuri NK, Heidelberger C. Studies on fluorinated pyrimidines. VIII. Further biochemical and metabolic investigations. J Biol Chem. 1959;234: 1255–62.

53. Lin J, Zhang W, Cheng J, Yang X, Zhu K, Wang Y, et al. A Pseudomonas T6SS effector recruits PQS-containing outer membrane vesicles for iron acquisition. Nat Commun. 2017;8: 14888. doi:10.1038/ncomms14888

54. Yurtsev EA, Chao HX, Datta MS, Artemova T, Gore J. Bacterial cheating drives the

population dynamics of cooperative antibiotic resistance plasmids. Mol Syst Biol. 2013;9: 683. doi:10.1038/msb.2013.39

55. Medaney F, Dimitriu T, Ellis RJ, Raymond B. Live to cheat another day□: bacterial dormancy facilitates the social exploitation of β -lactamases. ISME J. 2015;10: 778–787. doi:10.1038/ismej.2015.154

56. Kelsic ED, Zhao J, Vetsigian K, Kishony R. Counteraction of antibiotic production and degradation stabilizes microbial communities. Nature. 2015;521: 516–519. doi:10.1038/nature14485

57. Gellatly SL, Hancock REW. Pseudomonas aeruginosa: New insights into pathogenesis and host defenses. Pathog Dis. 2013;67: 159–173. doi:10.1111/2049-632X.12033

58. Beceiro A, Tomás M, Bou G. Antimicrobial resistance and virulence: A successful or deleterious association in the bacterial world? Clin Microbiol Rev. 2013;26: 185–230. doi:10.1128/CMR.00059-12

59. Lau GW, Hassett DJ, Ran H, Kong F. The role of pyocyanin in Pseudomonas aeruginosa infection. Trends Mol Med. 2004;10: 599–606. doi:10.1016/j.molmed.2004.10.002

60. Kümmerli R, Griffin AS, West S a, Buckling A, Harrison F. Viscous medium promotes cooperation in the pathogenic bacterium Pseudomonas aeruginosa. Proc Biol Sci. 2009;276: 3531–3538. doi:10.1098/rspb.2009.0861

61. Ross-Gillespie A, Gardner A, West SA, Griffin AS. Frequency dependence and cooperation: theory and a test with bacteria. Am Nat. 2007;170: 331–342. doi:10.1086/519860

62. Raymond B, West SA, Griffin AS, Bonsall MB. The dynamics of cooperative bacterial virulence in the field. Science (80-). 2012;337: 85–88. doi:10.1126/science.1218196

63. Garcia-Contreras R, Maeda T, Wood TK. Resistance to Quorum-Quenching Compounds. Appl Environ Microbiol. 2013;79: 6840–6846. doi:10.1128/AEM.02378-

13

64. Kalia VC, Wood TK, Kumar P. Evolution of resistance to quorum sensing inhibitors. Microb Ecol. 2014;68: 13–23. doi:10.1007/s00248-013-0316-y

65. Dandekar AA, Chugani S, Greenberg EP. Bacterial Quorum Sensing and Metabolic Incentives to Cooperate. Science. 2012;338: 264–266. doi:10.1126/science.1227289

66. Breidenstein EBM, de la Fuente-Núñez C, Hancock REW. Pseudomonas aeruginosa: all roads lead to resistance. Trends Microbiol. 2011;19: 419–426. doi:10.1016/j.tim.2011.04.005

67. Ling LL, Schneider T, Peoples AJ, Spoering AL, Engels I, Conlon BP, et al. A new antibiotic kills pathogens without detectable resistance. Nature. 2015;517: 455–459. doi:10.1038/nature14098

68. Perron GG, Zasloff M, Bell G. Experimental evolution of resistance to an antimicrobial peptide. Proc R Soc B Biol Sci. 2006;273: 251 LP-256. doi:10.1098/rspb.2005.3301

69. Hochberg ME, Jansen G. Bacteria: Assessing resistance to new antibiotics. Nature. 2015;519: 158. doi:10.1038/519158e

70. Bolger AM, Lohse M, Usadel B. Trimmomatic: a flexible trimmer for Illumina sequence data. Bioinformatics. 2014;30: 2114–2120. doi:10.1093/bioinformatics/btu170

71. Dodt M, Roehr J, Ahmed R, Dieterich C. FLEXBAR—Flexible Barcode and Adapter Processing for Next-Generation Sequencing Platforms. Biology (Basel). 2012;1: 895–905. doi:10.3390/biology1030895

72. Li H, Durbin R. Fast and accurate short read alignment with Burrows–Wheeler transform. Bioinformatics. 2009;25: 1754–1760. doi:10.1093/bioinformatics/btp324

73. McKenna A, Hanna M, Banks E, Sivachenko A, Cibulskis K, Kernytsky A, et al. The Genome Analysis Toolkit: a MapReduce framework for analyzing next-generation DNA sequencing data. Genome Res. 2010;20: 1297–1303. doi:10.1101/gr.107524.110

74. Cingolani P, Platts A, Wang LL, Coon M, Nguyen T, Wang L, et al. A program for

annotating and predicting the effects of single nucleotide polymorphisms, SnpEff. Fly (Austin). 2012;6: 80–92. doi:10.4161/fly.19695

75. Chessa JP, Petrescu I, Bentahir M, Van Beeumen J, Gerday C. Purification, physico-chemical characterization and sequence of a heat labile alkaline metalloprotease isolated from a psychrophilic Pseudomonas species. Biochim Biophys Acta - Protein Struct Mol Enzymol. 2000;1479: 265–274. doi:10.1016/S0167-4838(00)00018-2

76. Kahm M, Hasenbrink G, Ludwig J. grofit□: Fitting Biological Growth Curves with R. J Stat Softw. 2010;33. doi:10.18637/jss.v033.i07

77. Ritz C, Baty F, Streibig JC, Gerhard D. Dose-Response Analysis Using R. 2015; 1–13. doi:10.1371/journal.pone.0146021

Figure captions

Fig 1. Gallium and flucytosine affect both growth and pyoverdine production of *P. aeruginosa* in human serum (HS). Both anti-virulence drugs reduce growth of bacterial cultures in a dose-dependent manner (A, B), albeit following different patterns: gallium curbs bacterial growth only at relatively high concentrations (A), whereas flucytosine already reduces growth at low concentrations (B). Both drugs further affect pyoverdine production (C, D). When increasing gallium exposure, bacteria first upregulate pyoverdine production at intermediate drug concentrations, but then down-scale investment levels at high drug concentrations (C). In contrast, flucytosine administration leads to an almost complete abolishment of pyoverdine production even at the lowest drug concentration. All data are scaled relative to the drug-free treatment. Error bars denote standard errors of the mean across 6 (for flucytosine) and 18 (for gallium) replicates. Dose-response curves were fitted using either Weibull (for gallium) or Gompertz (for flucytosine) functions (see material and methods for details). Vertical lines indicate the drug concentrations used in the experimental evolution.

Fig 2. Population level growth and pyoverdine production after evolution in human serum. PAO1 cultures were exposed to either no treatment, low (50 µM) or high (280 µM) gallium, low (10 µg/ml) or high (140 µg/ml) flucytosine concentrations during a 20-day experimental evolution experiment in eight-fold replication. Following evolution, we assessed growth and pyoverdine production of evolved populations (displayed on the x-axis) and compared their performance relative to the untreated (gray solid line, set to 1) and treated ancestral wildtype (black dashed line). (A) Compared to the treated ancestral wildtype, growth of evolved populations significantly increased under all treatment regimes. Growth also increased in some but not all of the non-treatment lines. (B) Pyoverdine production of evolved populations significantly increased relative to the untreated ancestral wildtype under all conditions, also in the no treatment lines. This indicates that increased pyoverdine

production might be a general response to growth in human serum, which makes it difficult to disentangle resistance evolution from media adaptation. Error bars show the standard error of the mean across 5 independent replicates.

Fig 3. Changes in dose-response curves for evolved single clones indicate resistance evolution. 16 randomly picked clones, four per treatment, were exposed to a range of drug concentrations to test whether their dose-response altered during evolution compared to the ancestral wildtype (black circles and lines). (A and B) Growth dose-response curves under gallium treatment show that two evolved clones (GL2 and GH1) are significantly less inhibited than the ancestral wildtype. (C and D) Pyoverdine dose-response curves under gallium treatment show that two evolved clones (GL2 and GL3) make significantly more pyoverdine than the ancestral wildtype. (E and F) Growth dose-response curves under flucytosine treatment show that all evolved clones grow significantly better than the ancestral wildtype, and are in fact no longer affected by the drug. (G and H) Pyoverdine dose-response curves under flucytosine treatment show that all evolved clones produce significantly more pyoverdine than the ancestral wildtype, and are in fact no longer affected by the drug. Growth and pyoverdine production were measured after 24 h. For each clone, values are scaled relative to its performance in human serum without drugs (absolute values of pyoverdine and growth in the absence of treatment are reported in S3 Fig). We used spline functions to fit dose-response curves, and used the integral (area under the curve) to quantify the overall dose response of each clone across the concentration gradient. Error bars denote standard errors of the mean across 6 replicates. Asterisks represent significance levels: * = $p < 0.05$; *** = $p < 0.0001$, based on linear model with $df = 45$).

Fig 4. Upregulation of pyocyanin or protease production as potential bypassing mechanisms for iron acquisition under gallium treatment. The eight sequenced clones evolved under gallium treatments (low: 50 µM, high: 280 µM) were screened for their change

in the secretion of pyocyanin (A) and proteases (B) relative to the ancestral wildtype. Standard protocols were used for the phenotypic screens in drug free media (see Material and Methods for details). All values are corrected for cell number, and scaled relative to the ancestor wildtype (black line). We included the strains PAO1 Δ*rhlR* (deficient for pyocyanin production) and PAO1 Δ*lasR* (deficient for protease production) as negative controls in the respective assays (dashed lines). Error bars denote standard errors of the mean across 3 (for proteases) and 8 (for pyocyanin) replicates. Asterisks represent significance levels: * = $p < 0.05$; *** = $p < 0.0001$, based on ANOVA.

Fig 5. Upp is a non-essential enzyme, and mutations in its gene result in flucytosine resistance. (A) Flucytosine interferes with the pyrimidine metabolism in *P. aeruginosa.* The drug enters the cell through the transporter CodB (not shown), where it is first converted to fluorouracil by the cytosine deaminase CodA, and then to fluoro-UMP by the uracil phosphoribosyl-transferase Upp. Fluoro-UMP is a modified nucleotide precursor, the action of which results in RNA molecules with compromised functionality. Through an as yet unknown mechanism, fluoro-UMP also arrests pyoverdine synthesis in *P. aeruginosa*. Importantly, the nucleotide-precursor UMP can also be produced through an alternative *de-novo* pathway from the amino acids L-glutamine and L-aspartate, making Upp a non-essential enzyme in this bacterium. Experiments with the transposon mutant MPAO1 *Δupp* (deficient for Upp production) indeed demonstrate that the lack of Upp no longer affects strain growth (B) and pyoverdine production (C). This demonstrates that the inactivation of *upp* is a simple and efficient way to evolve resistance to flucytosine. Experiments were carried out in human serum across a range of flucytosine concentrations. Growth and pyoverdine production of MPAO1 *Δupp* (gray-dashed lines) and its corresponding wildtype MPAO1 (black-solid lines) were measured after 24 hours for each treatment separately in 6-fold replication. All values are scaled relative to the drug-free treatment. For statistical

analysis, we compared the integrals of the dose-response curves between the mutant and the wildtype strain.

Supporting information captions

S1 Fig. Human Serum is an iron limited media. To show that pyoverdine production is beneficial in human serum, we compared growth of *P. aeruginosa* PAO1 wildtype and of siderophore-deficient mutants PAO1 *ΔpvdD* and PAO1 *ΔpvdD ΔpchEF* in human serum with different supplements, which results in three different iron regimes. When adding only 50 mM HEPES to buffer the medium at physiological pH (middle panel) we observed that growth of siderophores mutants was significantly reduced compared to the wildtype (ANOVA, for PAO1 *ΔpvdD*: t_{15}= -7.47, p < 0.0001; for PAO1 *ΔpvdD ΔpchEF*: t_{15}= -6.87, p < 0.0001), confirming that human serum is an iron-limited media. To further increase iron limitation (left panel), we added the strong iron chelator human apo-transferrin (100 µg/ml) and its co-factor $NaHCO_3$ (20 mM); conversely to increase iron-availability in human serum we added 20 µM of iron chloride (right panel). We found that growth decreased when iron became more limiting (ANOVA, for human serum + transferrin: t_{49}= -25.26, p < 0.0001), while growth increased when extra iron was added (for human serum + iron chloride t_{49}= 14.60, p < 0.0001). However, the wildtype PAO1 grew significantly better compared to the siderophores mutants, in all three iron regimes (ANOVA, for PAO1 *ΔpvdD*: t_{49}= -8.12, p < 0.0001; for PAO1 *ΔpvdD ΔpchEF*: t_{49} = -7.91, p < 0.0001), confirming that siderophores are important for iron scavenging in human serum. All growth data are scaled relative to the wildtype growth in human serum supplemented with HEPES 50 mM (middle panel). Error bars denote standard errors of the mean across 6 replicates.

S2 Fig. Growth and pyoverdine production profiles of evolved single clones under treatment regimes. We were interested in examining the variation in growth and pyoverdine production profiles among evolved clones. For that purpose, we streaked out all evolved cultures on LB agar, and picked 5 random clones per evolved population. Overall, we isolated 160 clones, 40 clones per treatment. Single clones were tested under the treatment regime experienced during experimental evolution, and growth and pyoverdine production

were measured after 24 hours. Panels show growth and pyoverdine production of evolved clones relative to the untreated wildtype (grey line) under gallium (A, C) and flucytosine treatment (B, D). We found heterogeneous growth and pyoverdine patterns under all treatment regimes, suggesting diversification in evolving populations. Data points show means across three independent replicates. Dashed lines depict the mean growth or the mean pyoverdine production of the ancestral strain under treatment. Labeled single clones marked in red refer to the clones used for in-depth analysis and sequencing.

S3 Fig. Growth and pyoverdine production of evolved single clones in human serum with no treatment. We quantified the growth (A) and pyoverdine production (B) of the 16 evolved single clones we used for in-depth analysis and whole-genome sequencing. Specifically, we grew the clones for 24 hours in human serum and compared their performance to the ancestor wildtype in absence of the treatments. This allowed us to test for media adaptation. (A) We observed that some of the clones from both treatments showed significantly improved growth compared to the ancestral wildtype. This was the case for clones GL1 (t_{43} = 2.04, p = 0.0475), GL_4 (t_{43} = 2.04, p = 0.0475), GH_1 (t_{43} = 3.13, p = 0.0125), FL_1 (t_{43} = 5.88, p < 0.0001) and all clones evolved under high flucytosine (FH_1: t_{43} = 3.09, p = 0.0054; FH_2:, t_{43} = 3.03, p = 0.0054; FH_3: t_{43} = 4.38, p = 0.0002; FH_4, t_{43} = 2.82, p = 0.0071). Interestingly, two of the clones evolved under gallium low treatment showed reduced growth compared to PAO1 (GL_2: t_{43} = -3.35, p = 0.0033; GL_3: t_{43} = -3.36, p = 0.0033). (B) Regarding per capita pyoverdine production (pyoverdine fluorescence divided by growth), we found that two clones showed increased levels of pyoverdine production under gallium treatment (GL_1: t_{43} = 2.79, p = 0.0200; GL_4: t_{43} = 2.69, p = 0.0200), and three clones of the flucytosine high treatment did so too (FH_1: t_{43} = 2.43, p = 0.0356; FH_2: t_{43} = 2.29, p = 0.0356; for FH_4: t_{43} = 2.35, p = 0.0356). In contrast, there were also a number clones with significantly reduced pyoverdine production compared to PAO1 (GH_1: t_{43}= -3.14, p = 0.0045; GH_3: t_{43}= -3.10, p = 0.0045; GH_4: t_{43}= -3.46, p = 0.0045;

FL_4: t_{43}= -2.02, p=0.0488). All data are scaled relative to the ancestor wildtype. Error bars denote standard error of the mean across 6 replicates. Asterisks represent significance codes (* = p<0.05; ** = p<0.001, *** = p<0.0001 based on ANOVA, corrected for multiple pairwise comparison with the false discovery rate method).

S4 Fig. Alteration of the fluorescent properties of pyoverdine when bound to gallium. The fluorescent signal of pyoverdine becomes inflated when gallium binds to it [19]. To take this signal bias into account, we quantified the bias in fluorescence signal as a function of gallium concentration. Specifically, we supplemented iron-limited human serum with 200 µM of purified pyoverdine across a range of gallium concentrations (8 to 512 µM, as used for the main experiments). We found that the signal bias can be explained by a 3 parameters-logistic function. We used this function to correct for signal bias in all our analyses.

S1 Table. Effects of mutation on the Upp protein sequence of evolved single clones.

S2 Table. List of control strains used in this study.

S3 Table. Differences to the PAO1 reference genome shared among all sequenced evolved clones and the ancestor wildtype.

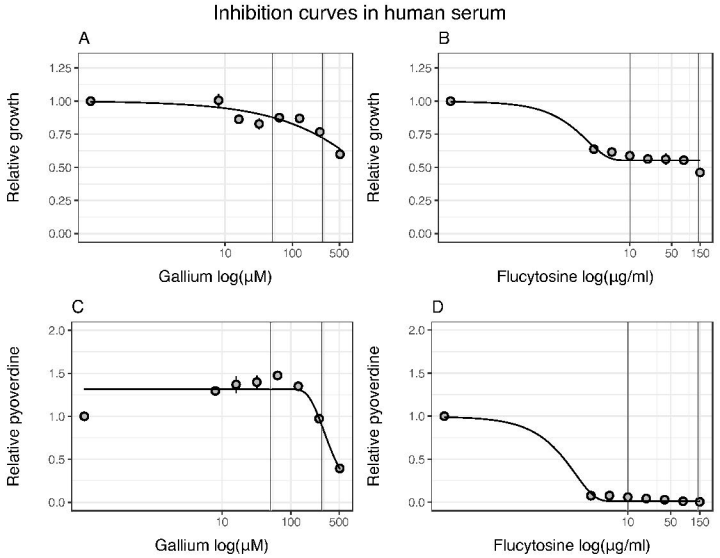
Inhibition curves in human serum
A
B
C
D
Relative growth
Relative pyoverdine
1.25
1.00
0.75
0.50
0.25
0.00
2.0
1.5
1.0
0.5
0.0
10
100
500
50
150
Gallium log(μM)
Flucytosine log(μg/ml)

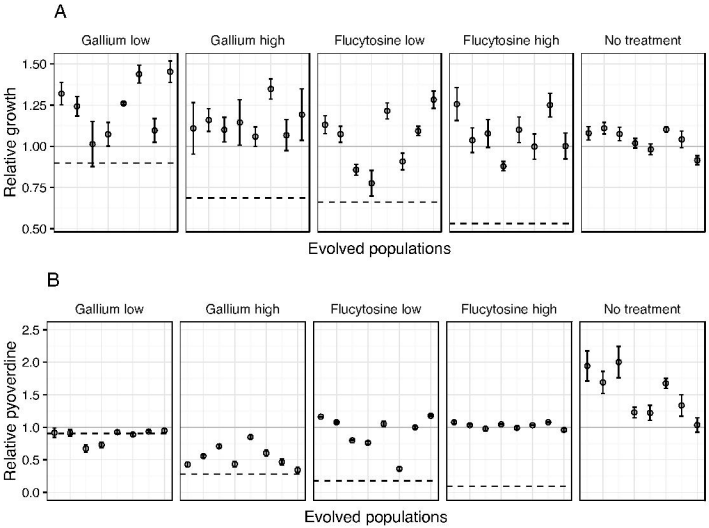
A
Gallium low
Gallium high
Flucytosine low
Flucytosine high
No treatment
Relative growth
1.50
1.25
1.00
0.75
0.50
Evolved populations
B
Gallium low
Gallium high
Flucytosine low
Flucytosine high
No treatment
Relative pyoverdine
2.5
2.0
1.5
1.0
0.5
0.0
Evolved populations

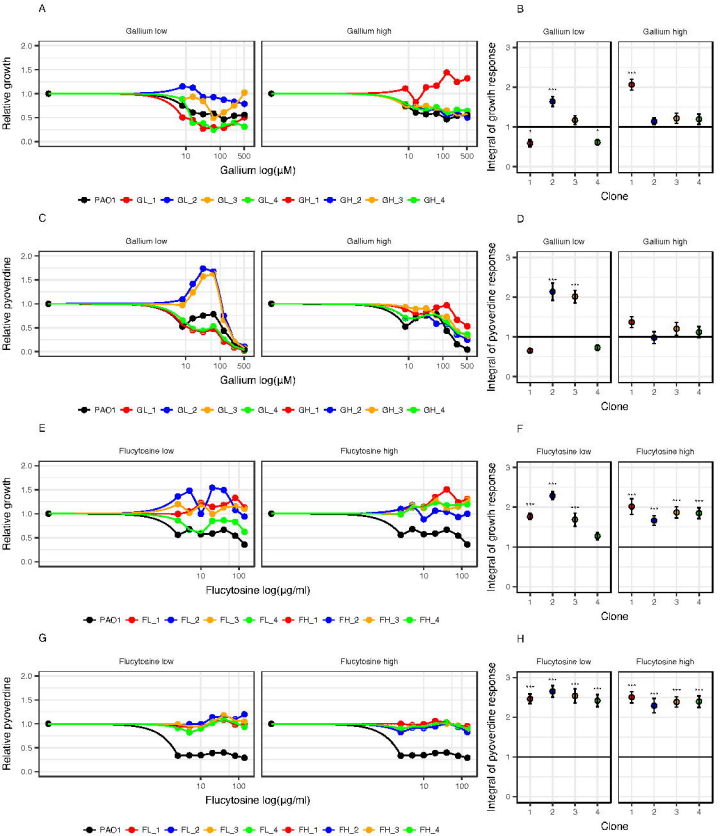
A
Gallium low
Gallium high
Relative growth
Gallium log(μM)
PAO1 GL_1 GL_2 GL_3 GL_4 GH_1 GH_2 GH_3 GH_4
B
Gallium low
Gallium high
Integral of growth response
Clone
C
Gallium low
Gallium high
Relative pyoverdine
Gallium log(μM)
PAO1 GL_1 GL_2 GL_3 GL_4 GH_1 GH_2 GH_3 GH_4
D
Gallium low
Gallium high
Integral of pyoverdine response
Clone
E
Flucytosine low
Flucytosine high
Relative growth
Flucytosine log(μg/ml)
PAO1 FL_1 FL_2 FL_3 FL_4 FH_1 FH_2 FH_3 FH_4
F
Flucytosine low
Flucytosine high
Integral of growth response
Clone
G
Flucytosine low
Flucytosine high
Relative pyoverdine
Flucytosine log(μg/ml)
PAO1 FL_1 FL_2 FL_3 FL_4 FH_1 FH_2 FH_3 FH_4
H
Flucytosine low
Flucytosine high
Integral of pyoverdine response
Clone

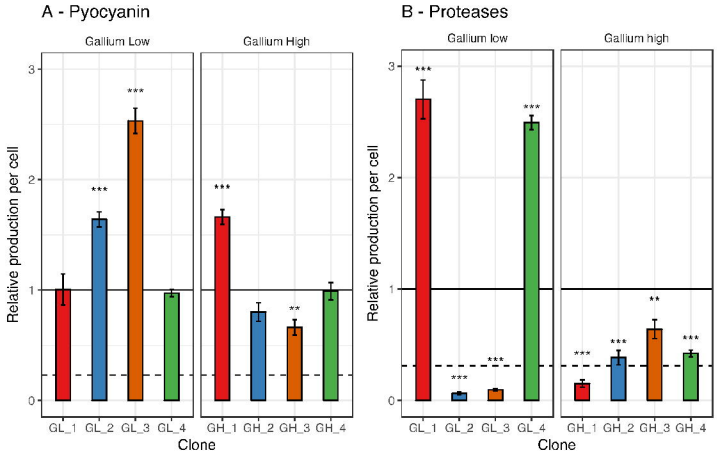
A - Pyocyanin
Gallium Low
Gallium High
Relative production per cell
Clone
GL_1
GL_2
GL_3
GL_4
GH_1
GH_2
GH_3
GH_4
B - Proteases
Gallium low
Gallium high

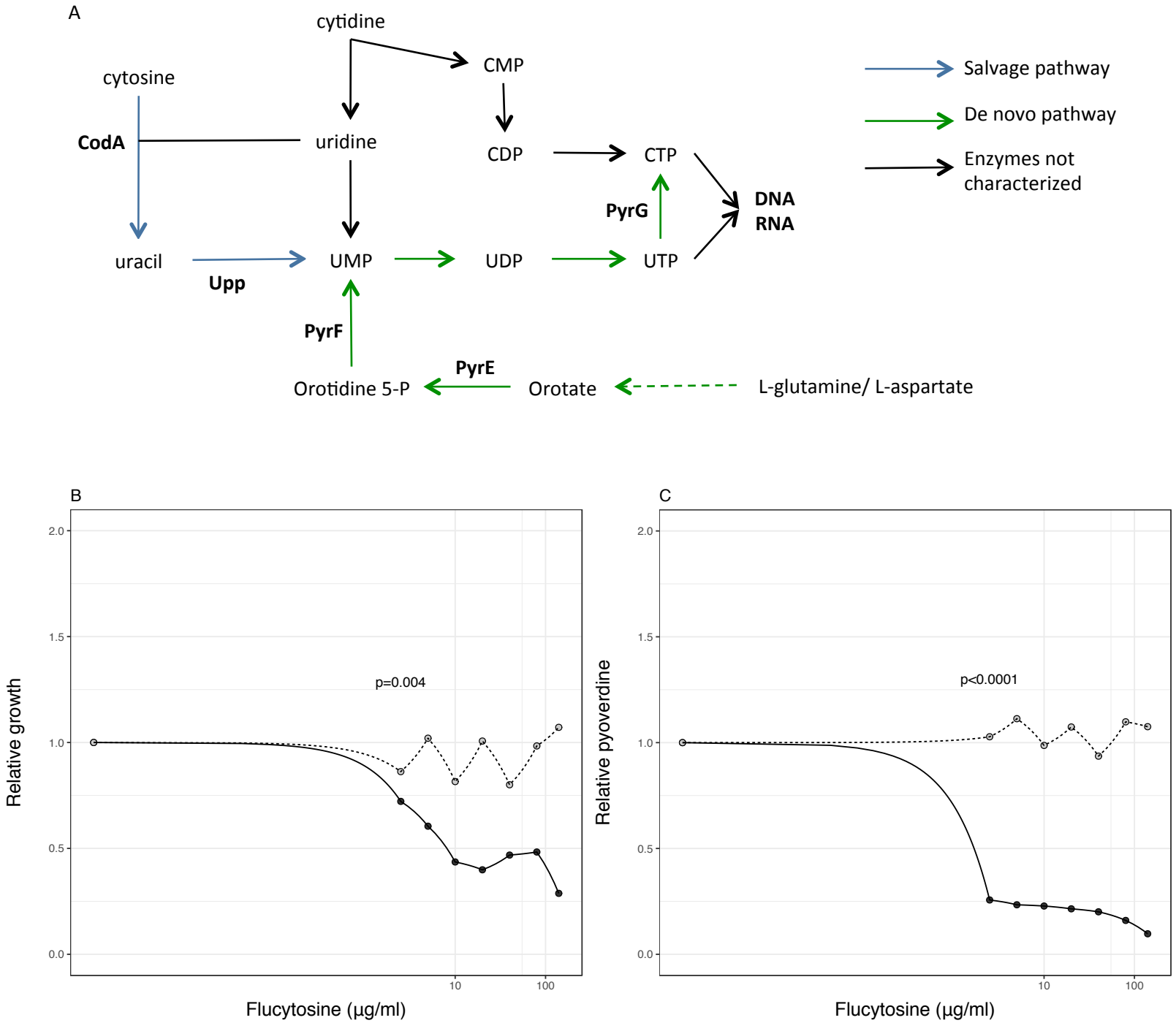
A
cytidine
CMP
cytosine
CodA
uridine
CDP
CTP
Salvage pathway
De novo pathway
Enzymes not characterized
PyrG
DNA
RNA
uracil
UMP
UDP
UTP
Upp
PyrF
PyrE
Orotidine 5-P
Orotate
L-glutamine/ L-aspartate
B
Relative growth
p=0.004
Flucytosine (µg/ml)
C
Relative pyoverdine
p<0.0001
Flucytosine (µg/ml)